Physica D 255 (2013) 1–11

Contents lists available at SciVerse ScienceDirect

Physica D

journal homepage: www.elsevier.com/locate/physd

On transverse stability of discrete line solitons

Dmitry E. Pelinovsky [a,b,*], Jianke Yang [c]

[a] Department of Mathematics and Statistics, McMaster University, Hamilton, Ontario, Canada, L8S 4K1
[b] Department of Applied Mathematics, Nizhny Novgorod State Technical University, Nizhny Novgorod, Russia
[c] Department of Mathematics and Statistics, University of Vermont, Burlington, VT 05401, USA

HIGHLIGHTS

- We develop rigorous analysis of transverse instability of discrete line solitons.
- We derive useful asymptotic approximations of unstable eigenvalues and eigenvalues of negative Krein signature.
- We illustrate rigorous results using numerical approximations.

ARTICLE INFO

Article history:
Received 4 October 2012
Received in revised form
9 February 2013
Accepted 26 March 2013
Available online 10 April 2013
Communicated by K. Promislow

Keywords:
Discrete NLS equations
Line solitons
Transverse stability

ABSTRACT

We obtain sharp criteria for transverse stability and instability of line solitons in the discrete nonlinear Schrödinger equations on one- and two-dimensional lattices near the anti-continuum limit. On a two-dimensional lattice, the fundamental line soliton is proved to be transversely stable (unstable) when it bifurcates from the X (Γ) point of the dispersion surface. On a one-dimensional (stripe) lattice, the fundamental line soliton is proved to be transversely unstable for both signs of transverse dispersion. If this transverse dispersion has the opposite sign to the discrete dispersion, the instability is caused by a resonance between isolated eigenvalues of negative energy and the continuous spectrum of positive energy. These results are obtained for focusing nonlinearity, and the results for defocusing nonlinearity can be deduced from a staggering transformation. When the line soliton is transversely unstable, asymptotic expressions for unstable eigenvalues are also derived. These analytical results are compared with numerical results and good agreement is obtained.

1. Introduction

One-dimensional solitons, when viewed in two spatial dimensions, become line solitons which are uniform along the line direction (called the transverse direction). Thus an important physical question is the transverse stability of line solitons to transverse perturbations. It is well known that in homogeneous media, line solitons in the nonlinear Schrödinger (NLS) equation and other related wave equations are always transversely unstable [1] (see also [2–4] for applications in optics and [5,6] for reviews). This instability has been observed in recent optical experiments [7–9].

In the presence of a one-dimensional (stripe) periodic potential, many line solitons are still transversely unstable [10,11]. To suppress this transverse instability, various techniques have been proposed [12–15]. In particular, it was shown numerically in [16,17] that when a one- or two-dimensional periodic potential is included in the continuous NLS equation, this transverse instability can be completely eliminated if the line soliton bifurcates from certain symmetry points of the dispersion surface. Similar suppression of transverse instability was also reported for line solitons in the discrete nonlinear Schrödinger (dNLS) equation on a two-dimensional square lattice [18,19].

In this article, we analytically investigate transverse stability of line solitons in the dNLS equations on two-dimensional (square) and one-dimensional (stripe) lattices. Near the anti-continuum limit, we derive sharp stability criteria for these discrete line solitons. On a two-dimensional lattice, we prove that the fundamental line soliton is transversely stable (unstable) when it bifurcates from the X (Γ) point of the dispersion surface. On a one-dimensional lattice, we prove that the fundamental line soliton is transversely unstable for both signs of transverse dispersion. These results are obtained under focusing nonlinearity, and the results with defocusing nonlinearity can be deduced from a staggering transformation. For unstable line solitons, their unstable eigenvalues are also derived asymptotically. In addition, we investigate the transverse stability of line solitons numerically both near the anti-continuum limit and away from it. Near the anti-continuum limit, the numerical results fully agree with the

* Corresponding author at: Department of Mathematics and Statistics, McMaster University, Hamilton, Ontario, L8S 4K1, Canada.
E-mail addresses: dmpeli@math.mcmaster.ca (D.E. Pelinovsky), jyang@math.uvm.edu (J. Yang).

0167-2789/$ – see front matter © 2013 Elsevier B.V. All rights reserved.
http://dx.doi.org/10.1016/j.physd.2013.03.011

analytical results. Away from the anti-continuum limit, we reveal additional bifurcations of unstable eigenvalues which cannot be captured by the theoretical analysis.

The main novelty of our article is the analytical determination of transverse stability or instability of discrete line solitons by the negative index theory [20–22]. In particular, near the anti-continuum limit, we are able to check analytically the assumptions of the negative index theory and to provide definite answers on the stability or instability of discrete line solitons. Another novelty of our article is the rigorous derivation of analytical approximations for the relevant eigenvalues responsible for transverse instabilities of discrete line solitons. In the case of one-dimensional (stripe) lattices, these analytical approximations deal with a delicate problem of a Hamilton–Hopf bifurcation of neutrally-stable eigenvalues embedded inside the continuous spectral band.

This article is organized as follows. In Section 2, we consider the transverse stability of discrete line solitons on a two-dimensional lattice. We show that the entire solution family bifurcating from the Γ point is transversely unstable, whereas the solution family bifurcating from the X point is transversely stable in the anti-continuum limit. In Section 3, we consider the transverse stability of discrete line solitons on a one-dimensional lattice, and show that they are always unstable. Numerical results and their comparison with the theory are reported in Section 4. Section 5 concludes the article with a discussion of open problems.

Before we start, we first introduce some mathematical notations which will be used in later analysis. If $\{\psi_n\}_{n\in\mathbb{Z}}$ is a bi-infinite sequence (i.e., a sequence which is infinite in both directions), and $\mathbb{Z}$ is the set of integers, then ψ denotes the vector for this sequence in some vector space such as $l^2(\mathbb{Z})$ or, more generally, $l^p(\mathbb{Z})$ for $p \geq 1$. Here $l^2(\mathbb{Z})$ denotes the space of bi-infinite squared-summable sequences with the norm

$$\|\psi\|_{l^2} \equiv \left(\sum_{n\in\mathbb{Z}} |\psi_n|^2\right)^{1/2}$$

and the inner product

$$\langle\psi, \varphi\rangle \equiv \sum_{n\in\mathbb{Z}} \bar{\psi}_n\varphi_n,$$

with the overbar for complex conjugation, and $l^p(\mathbb{Z})$ denotes the space of sequences with the norm

$$\|\psi\|_{l^p} \equiv \left(\sum_{n\in\mathbb{Z}} |\psi_n|^p\right)^{1/p}.$$

2. The case of two-dimensional lattices

In this section, we study transverse stability of line solitons in the dNLS equation on a two-dimensional lattice,

$$i\frac{du_{m,n}}{dt} + \epsilon(u_{m+1,n} + u_{m-1,n} + u_{m,n+1} + u_{m,n-1} - 4u_{m,n}) + |u_{m,n}|^2 u_{m,n} = 0, \tag{2.1}$$

where $(m, n) \in \mathbb{Z}^2$, $u_{m,n}$ are complex-valued amplitudes that depend on the evolution time t, and ϵ is the lattice-coupling constant. Here the sign of nonlinearity has been normalized to be unity through a scaling of ϵ and t. The anti-continuum limit of zero coupling between lattice sites ($\epsilon = 0$) was found to be very attractive for many analytical studies on the existence and stability of discrete solitons in the framework of the dNLS equation (see, e.g., [23,24]). Detailed accounts of mathematical results obtained in the anti-continuum limit can be found in books [25,26].

In the above dNLS equation, the defocusing case $\epsilon < 0$ can be mapped to the focusing case $\epsilon > 0$ by the staggering transformation

$$u_{m,n}(t) = (-1)^{m+n} v_{m,n}(t) e^{-8i\epsilon t}. \tag{2.2}$$

If u solves the dNLS equation (2.1), then v solves the same equation with ϵ replaced by $-\epsilon$. Thus, in what follows, we will consider the focusing case ($\epsilon > 0$) only.

The linear dispersion surface of the dNLS equation (2.1) is given by the function

$$\omega(k, p) = \epsilon(4 - 2\cos(k) - 2\cos(p)) = 4\epsilon\left[\sin^2\left(\frac{k}{2}\right) + \sin^2\left(\frac{p}{2}\right)\right],$$

where wavenumbers (k, p) reside in the first Brillouin zone $[-\pi, \pi] \times [-\pi, \pi]$. This dispersion relation can be derived by substituting the discrete Fourier modes $u_{m,n}(t) = e^{ikm+ipn-i\omega t}$ into the linear dNLS equation (2.1).

To understand bifurcations of stationary line solitons in Eq. (2.1), we need to classify the stationary points of the dispersion surface, where $\nabla\omega(k, p) = 0$. In the semi-open Brillouin zone $(-\pi, \pi] \times (-\pi, \pi]$, there are only four stationary points, which are commonly labeled as Γ, X, X', and M.

- Γ: $(k, p) = (0, 0)$ is the minimum point of the dispersion surface with $\omega(0, 0) = 0$;
- X: $(k, p) = (0, \pi)$ is a saddle point of the dispersion surface with $\omega(0, \pi) = 4\epsilon$;
- X': $(k, p) = (\pi, 0)$ is the other saddle point of the dispersion surface with $\omega(\pi, 0) = 4\epsilon$;
- M: $(k, p) = (\pi, \pi)$ is the maximum point of the dispersion surface with $\omega(\pi, \pi) = 8\epsilon$.

Discrete line solitons may bifurcate from any stationary point provided that the effective envelope NLS equation is focusing [26, Section 1.1.2]. Let us consider each of the possibilities. For definiteness, we assume that the line soliton is localized along the m-direction and uniform along the n-direction.

Γ: For $(k, p) = (0, 0)$, we substitute $u_{m,n}(t) = e^{i\mu^2 t}\psi_m$ and obtain the stationary 1D dNLS equation

$$-\mu^2\psi_m + \epsilon(\psi_{m+1} + \psi_{m-1} - 2\psi_m) + |\psi_m|^2\psi_m = 0, \tag{2.3}$$

which admits discrete solitons for any $\epsilon > 0$ and $\mu \neq 0$ [27,28]. Moreover, for fixed $\epsilon > 0$, the discrete soliton is approximated by the NLS soliton

$$\psi_m \to \sqrt{2}\mu\ \text{sech}\left(\frac{\mu m}{\sqrt{\epsilon}}\right) \quad \text{as } \mu \to 0. \tag{2.4}$$

This approximation was rigorously justified in the recent work [29] (see also [26, Section 2.3.2]).

X: For $(k, p) = (0, \pi)$, we substitute $u_{m,n}(t) = (-1)^n e^{i(\mu^2-4\epsilon)t}\psi_m$ and obtain the same stationary dNLS equation (2.3), which admits the discrete solitons for any $\epsilon > 0$ and $\mu \neq 0$.

X': For $(k, p) = (\pi, 0)$, we substitute

$$u_{m,n}(t) = (-1)^m e^{-i(\mu^2+4\epsilon)t}\psi_m$$

and obtain the stationary 1D dNLS equation

$$\mu^2\psi_m - \epsilon(\psi_{m+1} + \psi_{m-1} - 2\psi_m) + |\psi_m|^2\psi_m = 0. \tag{2.5}$$

This stationary equation admits no discrete solitons for any $\epsilon > 0$ [26, Lemma 3.10]. Indeed, by projecting Eq. (2.5) to ψ and denoting $(\Delta\psi)_m \equiv \psi_{m+1} + \psi_{m-1} - 2\psi_m$, we obtain a contradiction

$$\mu^2\|\psi\|_{l^2}^2 + \epsilon\langle\psi, (-\Delta)\psi\rangle + \|\psi\|_{l^4}^4 = 0,$$

since each term on the left side is positive definite.

M: For $(k,p)=(\pi,\pi)$, we substitute

$$u_{m,n}(t)=(-1)^{m+n}e^{-i(\mu^2+8\epsilon)t}\psi_m$$

and obtain the same stationary dNLS equation (2.5), which admits no discrete solitons for any $\epsilon>0$.

From the above analysis, we see that only two bifurcations of discrete line solitons occur and the bifurcation points are Γ and X. In the following, we will analyze transverse stability of these line solitons in the anti-continuum limit $\epsilon\to 0$ for fixed $\mu>0$ (or equivalently, $\mu\to\infty$ for fixed $\epsilon>0$).

Before the transverse-stability analysis in the anti-continuum limit, it is useful to recall the transverse-stability results in the opposite (continuum) limit that arise when $\epsilon\to\infty$ for fixed $\mu>0$ (or equivalently, $\mu\to 0$ for fixed $\epsilon>0$).

Γ: For $(k,p)=(0,0)$, we substitute

$$u_{m,n}(t)=U(X,Y,t)e^{i\mu^2 t},\quad X=\frac{m}{\sqrt{\epsilon}},\ Y=\frac{n}{\sqrt{\epsilon}}$$

into Eq. (2.1). Assuming smoothness of the envelope function $U(X,Y,t)$, we obtain an elliptic 2D NLS equation for $U(X,Y,t)$ as $\epsilon\to\infty$:

$$i\frac{\partial U}{\partial t}+\frac{\partial^2 U}{\partial X^2}+\frac{\partial^2 U}{\partial Y^2}+(|U|^2-\mu^2)U=0. \tag{2.6}$$

The line soliton (2.4) is transversely unstable in this elliptic NLS equation (2.6) due to neck-type instability (see [5,6] and references therein).

X: For $(k,p)=(0,\pi)$, we substitute

$$u_{m,n}(t)=(-1)^n U(X,Y,T)e^{i(\mu^2-4\epsilon)t},\quad X=\frac{m}{\sqrt{\epsilon}},\ Y=\frac{n}{\sqrt{\epsilon}}$$

into Eq. (2.1). Assuming smoothness of the envelope function $U(X,Y,t)$, we obtain a hyperbolic 2D NLS equation for $U(X,Y,t)$ as $\epsilon\to\infty$:

$$i\frac{\partial U}{\partial t}+\frac{\partial^2 U}{\partial X^2}-\frac{\partial^2 U}{\partial Y^2}+(|U|^2-\mu^2)U=0. \tag{2.7}$$

The line soliton (2.4) is also transversely unstable in this hyperbolic NLS equation (2.7) due to snaking-type instability (see [30,6] and references therein).

From reductions to 2D NLS equations (2.6) and (2.7), we see that discrete line solitons (2.4) are always transversely unstable in the continuum limit. Thus it is surprising that discrete line solitons were reported to be transversely stable far from the continuum limit when they bifurcate from the X point of the dispersion surface [18,16]. Line solitons bifurcated from the Γ point, however, remain transversely unstable for all values of ϵ (i.e., both near the continuum limit and away from it) [18,16]. Below we shall prove these numerical observations by rigorous spectral-stability analysis that relies on the count of eigenvalues of negative energy [20–22]. In addition, asymptotic expressions for unstable eigenvalues will also be derived in the anti-continuum limit.

2.1. Instability of line solitons bifurcating from the Γ point

Discrete line solitons bifurcating from the Γ point are of the form

$$u_{m,n}(t)=e^{i\mu^2 t}\psi_m, \tag{2.8}$$

where ψ satisfies the stationary 1D dNLS equation (2.3). It can be easily shown that $\{\psi_m\}_{m\in\mathbb{Z}}$ in these discrete solitons is real-valued (up to multiplication by $e^{i\alpha}$ for real α) [26, Lemma 3.11]. Perturbing these line solitons as

$$u_{m,n}(t)=e^{i\mu^2 t}\left[\psi_m+v_{m,n}(t)\right],$$

and substituting it into the dNLS equation (2.1), we obtain the linearized dNLS equation as

$$i\frac{dv_{m,n}}{dt}-\mu^2 v_{m,n}+\epsilon(v_{m+1,n}+v_{m-1,n}+v_{m,n+1}+v_{m,n-1}-4v_{m,n})+\psi_m^2(2v_{m,n}+\bar{v}_{m,n})=0.$$

For normal modes

$$\begin{aligned} v_{m,n}(t)&=e^{\lambda t+ipn}\left(U_m+iW_m\right),\\ \bar{v}_{m,n}(t)&=e^{\lambda t+ipn}\left(U_m-iW_m\right),\end{aligned} \tag{2.9}$$

we obtain the standard form of the eigenvalue problem

$$L_+(p)U=-\lambda W,\qquad L_-(p)W=\lambda U, \tag{2.10}$$

where $L_\pm(p)$ are p-dependent 1D discrete Schrödinger operators,

$$\begin{aligned}(L_+(p)U)_m &\equiv -\epsilon\left[U_{m+1}+U_{m-1}+2\cos(p)U_m-4U_m\right]\\ &\quad +\mu^2U_m-3\psi_m^2U_m,\\ (L_-(p)W)_m &\equiv -\epsilon[W_{m+1}+W_{m-1}+2\cos(p)W_m-4W_m]\\ &\quad +\mu^2W_m-\psi_m^2W_m.\end{aligned} \tag{2.11}$$

It is easy to see that eigenvalues λ in the above linear-stability problem always appear as quadruples $(\lambda,\bar{\lambda},-\lambda,-\bar{\lambda})$ when λ is complex or as pairs $(\lambda,-\lambda)$ when λ is real or purely imaginary.

Among the two parameters μ and ϵ in the above eigenvalue problem, the ratio ϵ/μ^2 is invariant with respect to a scaling transformation. The anti-continuum limit corresponds to the limit of $\epsilon/\mu^2\to 0$. Without loss of generality, we fix $\mu=1$ and consider small values of $\epsilon>0$ below.

We are interested in transverse stability of the *fundamental* line soliton ψ_m, which is positive for all $m\in\mathbb{Z}$ and confined to a single lattice site, say at $m=0$, in the anti-continuum limit $\epsilon\to 0$. Because the stationary equation (2.3) is analytic in ϵ and polynomial in ψ, whereas the difference operator is bounded, the dependence of ψ on ϵ is real analytic near $\epsilon=0$ [26, Theorem 3.8]. Using the regular perturbation method, we can easily obtain the power series expansion for ψ as

$$\psi_m=\delta_{m,0}+\epsilon(\delta_{m,1}+\delta_{m,0}+\delta_{m,-1})+\mathcal{O}(\epsilon^2), \tag{2.12}$$

where $\delta_{m,m'}$ is the Kronecker notation with $\delta_{m,m'}=1$ for $m=m'$ and 0 otherwise.

We shall now present the instability theorem for fundamental discrete line solitons bifurcating from the Γ point. This fundamental line soliton exists for any $\epsilon>0$ [27,28] (see also [26, Theorem 3.12]). Our instability theorem below applies to all values of $\epsilon>0$, except that the asymptotic expression for the unstable eigenvalue is valid only near the anti-continuum limit $\epsilon\to 0$.

Theorem 1. *Consider the fundamental discrete line soliton (2.8) bifurcating from the Γ point in the dNLS equation (2.1). For any $\epsilon>0$, there is $p_0(\epsilon)\in(0,\pi]$ such that for any $p\in(-p_0(\epsilon),p_0(\epsilon))\backslash\{0\}$ the linear-stability problem (2.10) admits a symmetric pair of real eigenvalues $\pm\lambda(\epsilon,p)$ with $\lambda(\epsilon,p)>0$. Hence this fundamental line soliton is transversely unstable for all $\epsilon>0$. In addition, $p_0(\epsilon)=\pi$ if $0<\epsilon<\frac{1}{2}$. Furthermore, for any $p\in[-\pi,\pi]$, the eigenvalue $\lambda(\epsilon,p)$ has the following asymptotic expansion in the anti-continuum limit,*

$$\lambda^2(\epsilon,p)=8\epsilon\sin^2\left(\frac{p}{2}\right)+\mathcal{O}(\epsilon^2)\quad \text{as } \epsilon\to 0. \tag{2.13}$$

Proof. We first rewrite operators $L_\pm(p)$ in (2.11) as

$$L_\pm(p)=L_\pm(0)+2\epsilon\left[1-\cos(p)\right].$$

These are bounded operators from $l^2(\mathbb{Z})$ to $l^2(\mathbb{Z})$, which have both continuous and discrete spectra.

The stationary equation (2.3) is simply $L_-(0)\psi = 0$. Because ψ is positive, 0 is at the bottom of the spectrum of $L_-(0)$, so that $L_-(0)$ is non-negative [31,32]. By the perturbation theory, $L_-(p)$ is strictly positive for any $p \in [-\pi, \pi] \setminus \{0\}$ and $\epsilon > 0$. On the other hand, $L_+(0)$ has at least one negative eigenvalue because

$$\langle L_+(0)\psi, \psi\rangle = -2\|\psi\|_{l^4}^4 < 0,$$

where $\|\psi\|_{l^4}^4 = \sum_{n\in\mathbb{Z}} |\psi_n|^4$. Moreover, in the limit $\epsilon \to 0$, only one negative eigenvalue of $L_+(0)$ exists, which is the eigenvalue -2 associated with the central site $m = 0$. By the variational arguments [27], this negative eigenvalue persists and remains the only negative eigenvalue of $L_+(0)$ for any $\epsilon > 0$. Since $L_+(p) \geq L_+(0)$, $L_+(p)$ has at most one negative eigenvalue and no zero eigenvalues. It follows from the stationary equation (2.3) with $\mu = 1$ that

$$\|\psi\|_{l^4}^4 = \|\psi\|_{l^2}^2 + \epsilon\langle\psi, (-\Delta)\psi\rangle \geq \|\psi\|_{l^2}^2,$$

where Δ is the 1D discrete Laplacian. Thus we obtain

$$\begin{aligned}\langle L_+(p)\psi, \psi\rangle &= -2\|\psi\|_{l^4}^4 + 2\epsilon\,[1-\cos(p)]\,\|\psi\|_{l^2}^2 \\ &\leq 2\,\{\epsilon\,[1-\cos(p)] - 1\}\,\|\psi\|_{l^2}^2,\end{aligned}$$

hence $L_+(p)$ admits a negative eigenvalue for any $p \in [-\pi, \pi]$ if $0 < \epsilon < \frac{1}{2}$ and for at least small p if $\epsilon > 0$ is arbitrary. In other words, for any $\epsilon > 0$, there is $p_0(\epsilon) \in (0, \pi]$ such that $L_+(p)$ has a negative eigenvalue for any $p \in (-p_0(\epsilon), p_0(\epsilon))$. Moreover, $p_0(\epsilon) = \pi$ at least for $0 < \epsilon < \frac{1}{2}$.

For $p = 0$, the linear eigenvalue problem (2.10) admits zero eigenvalue of algebraic multiplicity two for any $\epsilon > 0$ because $L_-(0)\psi = 0$ and

$$L_+(0)\frac{\partial\psi}{\partial(\mu^2)} = -\psi.$$

This zero eigenvalue is destroyed when $p \neq 0$ and this may cause instability when splitting of this double zero eigenvalue occurs along the real axis. Using the negative index theory [20–22,26], we obtain:

$$\begin{aligned}N_{\rm real}^- + N_{\rm imag}^- + N_{\rm comp} &= n(L_+(p)), \\ N_{\rm real}^+ + N_{\rm imag}^- + N_{\rm comp} &= n(L_-(p)),\end{aligned} \quad p \in [-\pi, \pi] \setminus \{0\}, \tag{2.14}$$

where $N_{\rm real}^+$ ($N_{\rm real}^-$) are the numbers of real positive eigenvalues λ with positive (negative) quadratic form $\langle L_+(p)U, U\rangle$ at the eigenvector (U, W) of the eigenvalue problem (2.10), $N_{\rm imag}^-$ is the number of purely imaginary eigenvalues λ with $\mathrm{Im}(\lambda) > 0$ and negative quadratic form $\langle L_+(p)U, U\rangle$, and $N_{\rm comp}$ is the number of complex eigenvalues λ with $\mathrm{Re}(\lambda) > 0$ and $\mathrm{Im}(\lambda) > 0$, counting their algebraic multiplicities. Note that eigenvalues contributing to $N_{\rm imag}^-$ are called eigenvalues with a negative Krein signature [21]. The eigenvalue-counting formula (2.14) follows directly from Theorem 4.5 of [26] because operators $L_\pm(p)$ have no zero eigenvalues for any $p \neq 0$.

The preceding computations show that $n(L_-(p)) = 0$, and $n(L_+(p)) = 1$ for $p \in (-p_0(\epsilon), p_0(\epsilon))$. In these cases, the index formula (2.14) yields

$$N_{\rm real}^- = 1, \qquad N_{\rm real}^+ = N_{\rm imag}^- = N_{\rm comp} = 0,$$

which proves the statement of Theorem 1 on transverse instability. It remains to justify the asymptotic expansion (2.13) for the real positive eigenvalue $\lambda(\epsilon, p)$ as $\epsilon \to 0$.

When $\epsilon = 0$, the spectral problem (2.10) with $\mu = 1$ has three points in the spectrum: $\lambda = 0$ of algebraic multiplicity two and $\lambda = \pm i$ of infinite algebraic multiplicity. Continuous spectral bands bifurcate from the points $\lambda = \pm i$ for $\epsilon \neq 0$. This bifurcation was studied in detail in the recent work [33], and no unstable eigenvalues arise in this bifurcation. We shall now calculate the splitting of the double zero eigenvalue for any fixed $p > 0$ and small $\epsilon > 0$, using the expansion (2.12) near the anti-continuum limit.

We rewrite the eigenvalue problem (2.10) with $\mu = 1$ at the central site $m = 0$ as follows:

$$\begin{aligned}&2U_0 + \epsilon\,[U_1 + U_{-1} + 2\cos(p)U_0 + 2U_0] + \mathcal{O}(\epsilon^2)U_0 = \lambda W_0, \\ &\epsilon\,[W_1 + W_{-1} + 2\cos(p)W_0 - 2W_0] + \mathcal{O}(\epsilon^2)W_0 = -\lambda U_0.\end{aligned}$$

By using the scaling transformation $U = \sqrt{\epsilon}\,\mathcal{U}$, $W = \mathcal{W}$, and $\lambda = \sqrt{\epsilon}\Lambda$, the system can be rewritten in the equivalent form:

$$\begin{aligned}&2\mathcal{U}_0 + \epsilon(\mathcal{U}_1 + \mathcal{U}_{-1} + 2\cos(p)\mathcal{U}_0 + 2\mathcal{U}_0) + \mathcal{O}(\epsilon^2)\mathcal{U}_0 = \Lambda\mathcal{W}_0, \\ &\mathcal{W}_1 + \mathcal{W}_{-1} + 2\cos(p)\mathcal{W}_0 - 2\mathcal{W}_0 + \mathcal{O}(\epsilon)\mathcal{W}_0 = -\Lambda\mathcal{U}_0.\end{aligned}$$

At the adjacent sites $m = \pm 1$, the linear eigenvalue problem (2.10) is

$$\begin{aligned}&\mathcal{U}_{\pm1} - \epsilon\,[\mathcal{U}_{\pm2} + \mathcal{U}_0 + 2\cos(p)\mathcal{U}_{\pm1} - 4\mathcal{U}_{\pm1}] \\ &\quad + \mathcal{O}(\epsilon^2)\mathcal{U}_{\pm1} = -\Lambda\mathcal{W}_{\pm1}, \\ &\mathcal{W}_{\pm1} - \epsilon\,[\mathcal{W}_{\pm2} + \mathcal{W}_0 + 2\cos(p)\mathcal{W}_{\pm1} - 4\mathcal{W}_{\pm1}] \\ &\quad + \mathcal{O}(\epsilon^2)\mathcal{W}_{\pm1} = \epsilon\Lambda\mathcal{U}_{\pm1},\end{aligned}$$

since $\psi_{\pm1}^2 = \mathcal{O}(\epsilon^2)$. Similar equations can be written for any $m \neq 0$.

For $\Lambda = \mathcal{O}(1)$, we have the reduction $\mathcal{U}_{\pm m} = \mathcal{O}(\epsilon^m)\mathcal{U}_0$ and $\mathcal{W}_{\pm m} = \mathcal{O}(\epsilon^m)\mathcal{W}_0$ for any $m \in \mathbb{N}$, which enables us to close the leading-order equations for $(\mathcal{U}_0, \mathcal{W}_0)$:

$$\begin{aligned}&2\mathcal{U}_0 + \mathcal{O}(\epsilon)\mathcal{U}_0 = \Lambda\mathcal{W}_0, \\ &[2\cos(p) - 2]\,\mathcal{W}_0 + \mathcal{O}(\epsilon)\mathcal{W}_0 = -\Lambda\mathcal{U}_0.\end{aligned}$$

After eliminating $\mathcal{W}_0$, we obtain the algebraic equation for Λ as

$$\Lambda^2 = 2(2 - 2\cos(p)) + \mathcal{O}(\epsilon) = 8\sin^2\left(\frac{p}{2}\right) + \mathcal{O}(\epsilon),$$

which then yields the asymptotic expansion (2.13). □

Remark 1. For any fixed $p \in [-\pi, \pi] \setminus \{0\}$, we obtain $\Lambda^2 > 0$ as $\epsilon \to 0$, which guarantees spectral instability of these discrete line solitons for small $\epsilon > 0$. Note that the asymptotic formula (2.13) is not uniform as $\epsilon \to 0$ and $p \to 0$, and a different perturbation theory is needed in the limit $p \to 0$ for fixed $\epsilon > 0$ (see [5,6] and references therein).

Remark 2. Using the resolvent analysis from [33], one can show that the continuous spectral bands are the two line-segments on the imaginary axis,

$$\begin{aligned}i\lambda &\in [-1 - 2\epsilon(3 - \cos(p)), -1 - 2\epsilon(1 - \cos(p))] \\ &\quad \cup [1 + 2\epsilon(1 - \cos(p)), 1 + 2\epsilon(3 - \cos(p))],\end{aligned}$$

whereas no discrete (isolated) eigenvalues bifurcate out from the point $\lambda = \pm i$ as $\epsilon \neq 0$.

Remark 3. In the continuous limit $\epsilon \to +\infty$, the discrete line solitons are asymptotically described by the elliptic NLS equation (2.6), where unstable real eigenvalues are restricted to the p-interval $(-p_0(\epsilon), p_0(\epsilon)) \setminus \{0\}$ with $p_0(\epsilon \to \infty) = \sqrt{3}$ (for $\mu = 1$) [5,6]. Therefore, $p_0(\epsilon) < \pi$ for sufficiently large positive ϵ.

2.2. Stability of line solitons bifurcating from the X point

Discrete line solitons bifurcating from the X point are of the form

$$u_{m,n}(t) = (-1)^n e^{i(\mu^2 - 4\epsilon)t}\psi_m, \tag{2.15}$$

where ψ is a real-valued solution of the stationary 1D dNLS equation (2.3). Notice that these solitons at adjacent lattice sites along the transverse n-direction are out-of-phase with each other, which contrasts with the line solitons bifurcating from the Γ point, where the solitons at adjacent lattice sites along the transverse direction are in phase with each other.

Linearizing the dNLS equation (2.1) around this solution, we substitute

$$u_{m,n}(t) = (-1)^n e^{i(\mu^2-4\epsilon)t}\left[\psi_m + v_{m,n}(t)\right],$$

and obtain the linearized dNLS equation

$$i\frac{dv_{m,n}}{dt} - \mu^2 v_{m,n} + \epsilon(v_{m+1,n} + v_{m-1,n} - v_{m,n+1} - v_{m,n-1}) + \psi_m^2(2v_{m,n} + \bar{v}_{m,n}) = 0.$$

For normal modes (2.9), we obtain the eigenvalue problem

$$L_+(p)U = -\lambda W, \qquad L_-(p)W = \lambda U, \tag{2.16}$$

where

$$\begin{aligned}(L_+(p)U)_m &\equiv -\epsilon\,[U_{m+1} + U_{m-1} - 2\cos(p)U_m] + \mu^2 U_m - 3\psi_m^2 U_m,\\ (L_-(p)W)_m &\equiv -\epsilon\,[W_{m+1} + W_{m-1} - 2\cos(p)W_m] + \mu^2 W_m - \psi_m^2 W_m.\end{aligned} \tag{2.17}$$

Again, we are interested in transverse stability of the fundamental line soliton ψ which is positive and given by the power series expansion (2.12) in the anti-continuum limit $\epsilon \to 0$. As before, we will fix $\mu = 1$ without loss of generality. The next theorem guarantees stability of this fundamental discrete line soliton for small values of ϵ.

Note that, although the operators $L_\pm(p)$ in (2.17) are only different from the operators $L_\pm(p)$ in (2.11) by the diagonal terms (uniform in m), the stability result of the next theorem is very different from the instability result of Theorem 1. In particular, these two results are not related to each other by a staggering transformation.

Theorem 2. *Consider the fundamental discrete line soliton (2.15) bifurcating from the X point in the dNLS equation (2.1). There exists $\epsilon_0 > 0$ such that for any $\epsilon \in (0, \epsilon_0)$ and $p \in [\pi, \pi]$, the linear-stability problem (2.16) does not admit any unstable eigenvalues, thus the fundamental line soliton for small values of ϵ is transversely stable. This stable line soliton possesses a pair of discrete imaginary eigenvalues $\pm i\omega(\epsilon, p)$ of negative Krein signature. Moreover, for any $p \in [-\pi, \pi]$ and small ϵ, this eigenvalue $\omega(\epsilon, p)$ has the following asymptotic expression,*

$$\omega^2(\epsilon, p) = 8\epsilon\sin^2\left(\frac{p}{2}\right) + \mathcal{O}(\epsilon^2) \quad \text{as } \epsilon \to 0. \tag{2.18}$$

Proof. We first rewrite operators $L_\pm(p)$ in (2.17) as

$$L_\pm(p) = L_\pm(0) - 2\epsilon\,[1 - \cos(p)].$$

Because $L_-(0)\psi = 0$ and ψ is positive, 0 is the lowest eigenvalue of $L_-(0)$ for any $\epsilon > 0$ [31,32]. By perturbation theory, $L_-(p)$ has exactly one negative eigenvalue for any $p \in [-\pi, \pi]\setminus\{0\}$ and small positive ϵ. On the other hand, since ψ and $L_+(0)$ for the line soliton (2.15) are the same as those for the line soliton (2.8), the variational arguments from [27] imply that $L_+(0)$ has exactly one negative eigenvalue and no zero eigenvalue for any $\epsilon > 0$. Therefore, $L_+(p)$ has a single negative eigenvalue for any $p \in [-\pi, \pi]$ and small positive ϵ.

For any $p \neq 0$, we again use the eigenvalue-counting formula (2.14), which equally applies to the linear eigenvalue problem (2.16). The preceding computation shows that there is $\epsilon_0 > 0$ such that $n(L_-(p)) = 1$ and $n(L_+(p)) = 1$ for any $\epsilon \in (0, \epsilon_0)$ and $p \in [-\pi, \pi] \setminus \{0\}$. Since eigenvalues in the spectral problem (2.16) appear as quadruples $(\lambda, \bar{\lambda}, -\lambda, -\bar{\lambda})$ for complex λ^2 and as pairs $\pm\lambda$ for real λ^2 and since the zero eigenvalue for $p = 0$ has algebraic multiplicity two, this zero eigenvalue splits along the real or imaginary axis as a pair of simple eigenvalues for $p \neq 0$. Combining this with the eigenvalue-counting formula (2.14), we easily see that this splitting occurs along the imaginary axis, and for any $\epsilon \in (0, \epsilon_0)$ and $p \in [-\pi, \pi] \setminus \{0\}$,

$$N_{\text{imag}}^- = 1, \qquad N_{\text{real}}^+ = N_{\text{real}}^- = N_{\text{comp}} = 0,$$

which proves the transverse-stability statement in Theorem 2. Note that the imaginary eigenvalues of negative Krein signature persist on the imaginary axis, unless they coalesce with other eigenvalues of positive Krein signature or continuous spectral bands.

Next we prove the asymptotic expansion (2.18) for the imaginary eigenvalue $i\omega(\epsilon, p)$ as $\epsilon \to 0$. When $\epsilon = 0$, the spectral problem (2.16) with $\mu = 1$ has three points in the spectrum: $\lambda = 0$ of algebraic multiplicity two and $\lambda = \pm i$ of infinite algebraic multiplicity. For small ϵ, we only need to compute the splitting of the double zero eigenvalue for any fixed $p \in [-\pi, \pi]$, using the expansion (2.12) near the anti-continuum limit.

Repeating the perturbation expansions and using the scaling transformation $U = \sqrt{\epsilon}\,\mathcal{U}$, $W = \mathcal{W}$, and $\lambda = \sqrt{\epsilon}\,\Lambda$, we obtain the linear eigenvalue problem at the central site $m = 0$:

$$\begin{aligned}&2\mathcal{U}_0 + \epsilon\,[\mathcal{U}_1 + \mathcal{U}_{-1} - 2\cos(p)\mathcal{U}_0 + 6\mathcal{U}_0] + \mathcal{O}(\epsilon^2)\mathcal{U}_0 = \Lambda\mathcal{W}_0,\\ &\mathcal{W}_1 + \mathcal{W}_{-1} - 2\cos(p)\mathcal{W}_0 + 2\mathcal{W}_0 + \mathcal{O}(\epsilon)\mathcal{W}_0 = -\Lambda\mathcal{U}_0.\end{aligned}$$

Similar to the proof of Theorem 1, for $\Lambda = \mathcal{O}(1)$, we have the reduction $\mathcal{U}_{\pm m} = \mathcal{O}(\epsilon^m)\mathcal{U}_0$ and $\mathcal{W}_{\pm m} = \mathcal{O}(\epsilon^m)\mathcal{W}_0$ for any $m \in \mathbb{N}$, hence the above equations yield

$$\Lambda^2 = -2\,[2 - 2\cos(p)] + \mathcal{O}(\epsilon) = -8\sin^2\left(\frac{p}{2}\right) + \mathcal{O}(\epsilon),$$

which yields the asymptotic expansion (2.18). □

Remark 4. For any $p \in [-\pi, \pi] \setminus \{0\}$ and small values of ϵ, we get $\Lambda^2 < 0$, which gives imaginary eigenvalues $\pm i\omega(\epsilon, p)$. It is easy to see that these imaginary eigenvalues have negative Krein signature, meaning that the quadratic form $\langle L_+(p)U, U\rangle$ at the eigenvector (U, W) is negative. For small values of ϵ, these imaginary eigenvalues are bounded away from the continuous spectrum bifurcating out of the points $\pm i$, which guarantees spectral stability of discrete line solitons for small positive ϵ.

Remark 5. Using the resolvent analysis from [33], one can show that the continuous spectral bands are located at the two segments on the imaginary axis:

$$\begin{aligned}i\lambda \in\ &[-1 - 2\epsilon(1 + \cos(p)), -1 + 2\epsilon(1 - \cos(p))]\\ &\cup[1 - 2\epsilon(1 - \cos(p)), 1 + 2\epsilon(1 + \cos(p))],\end{aligned}$$

and no discrete (isolated) eigenvalues bifurcate out from the points $\lambda = \pm i$ as $\epsilon \to 0$.

Remark 6. In the continuum limit $\epsilon \to +\infty$, discrete line solitons (2.15) from the X point in Eq. (2.1) are asymptotically described by the hyperbolic NLS equation (2.7), where line solitons are transversely unstable for any nonzero transverse wavenumber p [30,6]. Hence unstable eigenvalues must appear for these discrete line solitons at sufficiently large positive ϵ. These unstable eigenvalues can appear through collisions of imaginary eigenvalues of negative Krein signature with the continuous spectral band or with additional imaginary eigenvalues of positive Krein signature.

3. The case of one-dimensional (stripe) lattices

In this section, we consider transverse stability of line solitons in the dNLS equation on a one-dimensional (stripe) lattice with continuous transverse dispersion. This problem arises in nonlinear fiber arrays [34–36] and optically-induced stripe lattices [17]. The mathematical model for this problem is

$$i\frac{\partial u_m}{\partial t} + \epsilon(u_{m+1} + u_{m-1} - 2u_m) + \kappa\frac{\partial^2 u_m}{\partial y^2} + |u_m|^2 u_m = 0, \tag{3.1}$$

where $m \in \mathbb{Z}$, the complex variable u_m depends on the evolution time t and the transverse coordinate y. Here the sign of nonlinearity has been normalized to be unity through a scaling of ϵ, κ and t. By the staggering transformation

$$u_m(y,t) = (-1)^m v_m(y,t) e^{-4i\epsilon t}, \tag{3.2}$$

we can map the dNLS equation (3.1) for u with $\epsilon < 0$ to the same equation for v with $\epsilon > 0$. Thus we set $\epsilon > 0$ below but consider both positive and negative values of the transverse dispersion parameter κ. Through a scaling of y, we normalize κ so that $\kappa = \pm 1$.

Transverse instability of line solitons was reported in [17] for $\kappa = -1$ and any $\epsilon > 0$. We shall prove this numerical observation by rigorous study of spectral stability. We shall also study the case $\kappa = +1$ for completeness.

First, by inserting the discrete Fourier modes $u_m(y,t) = e^{ikm - i\omega t}$ into the linear dNLS equation (3.1), we find that the discrete-dispersion relation is

$$\omega(k) = 2\epsilon\left[1 - \cos(k)\right],$$

where the wavenumber k is in the first Brillouin zone $k \in [-\pi, \pi]$. For $\epsilon > 0$, discrete line solitons bifurcate from the minimum of this dispersion curve towards negative values of ω. Therefore the discrete line solitons are of the form

$$u_m(y,t) = e^{i\mu^2 t}\psi_m, \tag{3.3}$$

where ψ is a real-valued solution of the stationary 1D dNLS equation (2.3). Linearizing around this solution, we substitute

$$u_m(y,t) = e^{i\mu^2 t}\left[\psi_m + v_m(y,t)\right]$$

into the dNLS equation (3.1) and obtain the linearized dNLS equation

$$i\frac{\partial v_m}{\partial t} - \mu^2 v_m + \epsilon(v_{m+1} + v_{m-1} - 2v_m) + \kappa\frac{\partial^2 v_m}{\partial y^2} + \psi_m^2(2v_m + \bar{v}_m) = 0.$$

For the normal mode

$$v_m(y,t) = e^{\lambda t + ipy}\left(U_m + iW_m\right),$$
$$\bar{v}_m(y,t) = e^{\lambda t + ipy}\left(U_m - iW_m\right),$$

we obtain the linear-stability eigenvalue problem

$$L_+(p)U = -\lambda W, \qquad L_-(p)W = \lambda U, \tag{3.4}$$

where

$$\begin{aligned} (L_+(p)U)_m &\equiv -\epsilon(U_{m+1} + U_{m-1} - 2U_m) + (\mu^2 + \kappa p^2)U_m - 3\psi_m^2 U_m, \\ (L_-(p)W)_m &\equiv -\epsilon(W_{m+1} + W_{m-1} - 2W_m) + (\mu^2 + \kappa p^2)W_m - \psi_m^2 W_m. \end{aligned} \tag{3.5}$$

As before, we set $\mu = 1$ by variable rescaling and consider the fundamental line soliton represented by the power series expansion (2.12) for small ϵ.

When $\epsilon = 0$, the eigenvalue problem (3.4) with $\mu = 1$ has four points in the spectrum: two simple eigenvalues at $\lambda = \pm\sqrt{\kappa p^2(2 - \kappa p^2)}$ and two other eigenvalues of infinite algebraic multiplicities at $\lambda = \pm i(1 + \kappa p^2)$.

If $\kappa = 1$, the simple eigenvalues $\lambda = \pm p\sqrt{2 - p^2}$ are real for $0 < p^2 < 2$, thus the discrete line soliton (3.3) is transversely unstable even in the unperturbed ($\epsilon = 0$) case. These real eigenvalues persist for small ϵ. The following theorem shows that the transverse instability of discrete line solitons (3.3) with $\kappa = 1$ holds for any $\epsilon > 0$.

Theorem 3. *Consider the fundamental discrete line soliton (3.3) in the dNLS equation (3.1) with $\kappa = 1$. For any $\epsilon > 0$, there is $p_0(\epsilon) > 0$ such that for any $p \in (-p_0(\epsilon), p_0(\epsilon)) \setminus \{0\}$ the linear-stability problem (3.4) admits a pair of real eigenvalues $\pm\lambda(\epsilon, p)$ with $\lambda(\epsilon, p) > 0$, thus this line soliton is transversely unstable. In addition, for small ϵ, $p_0(\epsilon)$ and $\lambda(\epsilon, p)$ are given asymptotically by*

$$\begin{aligned} p_0(\epsilon) &= \sqrt{2} + \mathcal{O}(\epsilon), \\ \lambda(\epsilon, p) &= p\sqrt{2 - p^2} + \mathcal{O}(\epsilon) \quad \text{as } \epsilon \to 0. \end{aligned} \tag{3.6}$$

Proof. We first rewrite operators $L_\pm(p)$ in (3.5) as

$$L_\pm(p) = L_\pm(0) + p^2.$$

Similar to the proof of Theorem 1, we can see that $L_-(p)$ is strictly positive for any $p \neq 0$ and $\epsilon \geq 0$. On the other hand, for any $\epsilon \geq 0$, $L_+(0)$ has a single negative eigenvalue $-\beta$, where $\beta > 0$. In particular, when $\epsilon = 0$, the negative eigenvalue with $\beta = 2$ is associated with the central site $m = 0$. Thus by denoting $p_0(\epsilon) \equiv \sqrt{\beta}$, we see that $L_+(p)$ has exactly one negative eigenvalue for $p \in (-p_0(\epsilon), p_0(\epsilon))$ and is strictly positive for any $|p| > p_0(\epsilon)$. The eigenvalue-counting formula (2.14) then yields that when $p \in (-p_0(\epsilon), p_0(\epsilon)) \setminus \{0\}$,

$$N_{\text{real}}^- = 1, \qquad N_{\text{real}}^+ = N_{\text{imag}}^- = N_{\text{comp}} = 0.$$

The asymptotic expansions (3.6) directly follow from the preceding computations at $\epsilon = 0$ and the analyticity of the linear eigenvalue problem (3.4) in ϵ. □

Remark 7. The asymptotic expansion $\lambda(\epsilon, p) = p\sqrt{2 - p^2} + \mathcal{O}(\epsilon)$ works equally well for $|p| > p_0(\epsilon)$, where this $\lambda(\epsilon, p)$ is purely imaginary. These imaginary eigenvalues have positive Krein signature and are bounded away from the continuous spectrum located at

$$i\lambda \in [-(1 + p^2 + 4\epsilon), -(1 + p^2)] \cup [1 + p^2, 1 + p^2 + 4\epsilon].$$

If $\kappa = -1$ and $\epsilon = 0$, the simple eigenvalues $\lambda = \pm ip\sqrt{2 + p^2}$ are purely imaginary, so are the eigenvalues $\lambda = \pm i(1 - p^2)$ of infinite algebraic multiplicities. These eigenvalue branches intersect at $p = \pm p_c$, where $p_c = \frac{1}{2}$. When $p \neq \pm p_c$ and $0 < \epsilon \ll 1$, the simple eigenvalues persist on $i\mathbb{R}$, whereas two continuous spectral bands bifurcate from the non-simple eigenvalues $\lambda = \pm i(1 - p^2)$ along the two segments on $i\mathbb{R}$ as

$$i\lambda \in [1 - p^2, 1 - p^2 + 4\epsilon] \cup [-(1 - p^2 + 4\epsilon), -(1 - p^2)].$$

However, when $p = \pm p_c$ and $0 < \epsilon \ll 1$, a resonance occurs between these simple and non-simple eigenvalues, and as a consequence, complex (unstable) eigenvalues bifurcate out. Notice that the simple eigenvalues $\lambda = \pm ip\sqrt{2 + p^2}$ have negative Krein signature, whereas the non-simple eigenvalues $\lambda = \pm i(1 - p^2)$ have positive Krein signature. This bifurcation of complex eigenvalues due to the collision of eigenvalues with opposite Krein

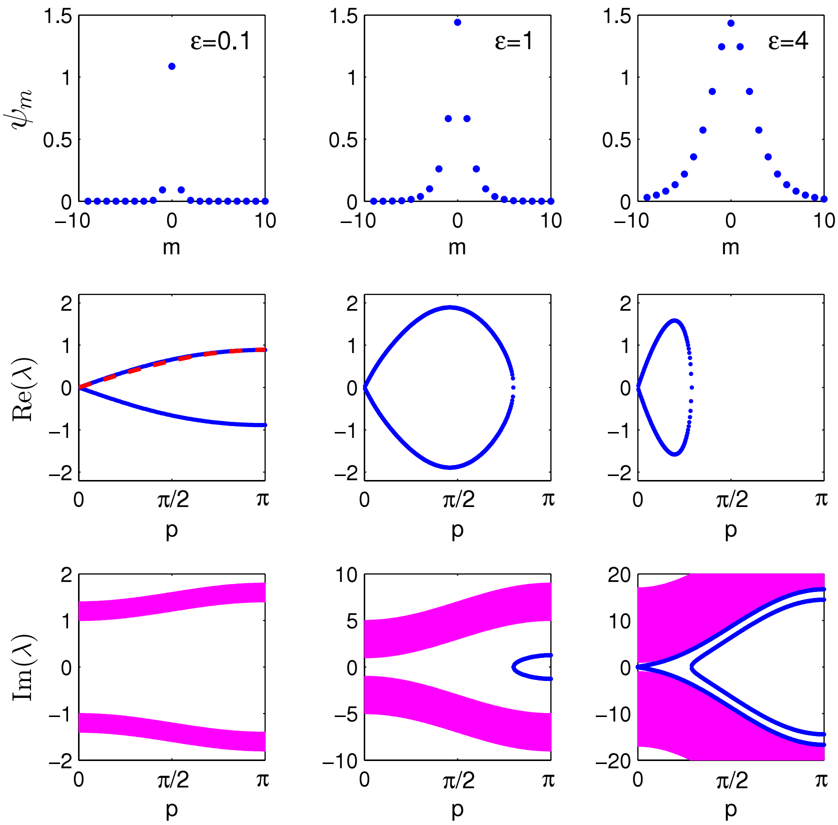

Fig. 1. Numerical results for discrete line solitons (2.8) bifurcating from the Γ point of the dNLS equation (2.1) on a two-dimensional lattice. Upper row: profiles of discrete line solitons ψ_m; middle row: real parts of eigenvalues λ of the spectral stability problem (2.10) versus the transverse wavenumber p; lower row: imaginary parts of eigenvalues λ versus p (the shaded pink region is the continuous spectrum). Left column: $\epsilon = 0.1$; middle column: $\epsilon = 1$; right column: $\epsilon = 4$. The red dashed line in the middle left panel is the leading-order analytical approximation (2.13) in Theorem 1. (For interpretation of the references to colour in this figure legend, the reader is referred to the web version of this article.)

signatures is a common phenomenon in Hamiltonian systems [21,37].

The following theorem guarantees instability of discrete line solitons (3.3) in the dNLS equation (3.1) with $\kappa = -1$ for small values of $\epsilon > 0$. This instability is caused by complex eigenvalues with small real parts, and it occurs for intermediate values of transverse wavenumbers p.

Theorem 4. *Consider the fundamental discrete line soliton (3.3) in the dNLS equation (3.1) with $\kappa = -1$. There exists $\epsilon_0 > 0$ such that for any $\epsilon \in (0, \epsilon_0)$, there exist $p_c^{\pm}(\epsilon)$ with ordering $0 < p_c^-(\epsilon) < p_c^+(\epsilon) < +\infty$, so that for any $|p| \in (p_c^-(\epsilon), p_c^+(\epsilon))$ the linear-stability problem (3.4) admits a quartet of complex eigenvalues $\pm\lambda(\epsilon, p), \pm\bar{\lambda}(\epsilon, p)$ with $\mathrm{Re}\lambda(\epsilon, p) > 0$ and $\mathrm{Im}\lambda(\epsilon, p) > 0$. In addition, when $\epsilon \to 0$, $p_c^{\pm}(\epsilon)$ and $\lambda(\epsilon, p)$ are given asymptotically by*

$$p_c^{\pm}(\epsilon) = \frac{1}{2} + \frac{\epsilon}{2}\left(1 \pm \frac{\sqrt{15}}{2}\right) + \mathcal{O}(\epsilon^2), \tag{3.7}$$

and

$$\lambda(\epsilon, p) = \frac{3}{4}i + \frac{i\epsilon}{15}(14 + 17\delta) + \frac{2\epsilon}{15}\sqrt{15 - 4(1 - 2\delta)^2} + \mathcal{O}(\epsilon^2), \tag{3.8}$$

where $\delta \equiv \epsilon^{-1}(p^2 - \frac{1}{4}) = \mathcal{O}(1)$. Furthermore, the most unstable eigenvalue $\lambda_{\max}(\epsilon)$ occurs at the transverse wavenumbers $\pm p_{\max}(\epsilon)$, where $\lambda_{\max}(\epsilon)$ and $p_{\max}(\epsilon)$ are given by

$$\lambda_{\max}(\epsilon) = \frac{3}{4}i + \epsilon\left(\frac{2}{\sqrt{15}} + \frac{3}{2}i\right) + \mathcal{O}(\epsilon^2), \quad p_{\max} = \frac{1}{2} + \frac{1}{2}\epsilon + \mathcal{O}(\epsilon^2). \tag{3.9}$$

Proof. Modifying the arguments from the proof of Theorem 3, we have now

$$L_{\pm}(p) = L_{\pm}(0) - p^2.$$

Therefore, for sufficiently small ϵ, there is $p_0(\epsilon) > 0$ such that the operators $L_{\pm}(p)$ have exactly one negative eigenvalue for all $p \in (-p_0(\epsilon), p_0(\epsilon)) \setminus \{0\}$. Note that $p_0(\epsilon) = 1 + \mathcal{O}(\epsilon)$ as $\epsilon \to 0$.

The eigenvalue-counting formula (2.14) yields now

$$N_{\text{imag}}^- + N_{\text{comp}} = 1, \qquad N_{\text{real}}^+ = N_{\text{real}}^- = 0, \quad p \in (-p_0(\epsilon), p_0(\epsilon)) \setminus \{0\}.$$

The preceding computations and the analyticity of the linear eigenvalue problem (3.4) in ϵ imply that for sufficiently small ϵ, there are $p_c^{\pm}(\epsilon)$ with ordering $0 < p_c^-(\epsilon) < p_c^+(\epsilon) < p_0(\epsilon)$ such that

$$N_{\text{imag}}^- = 1, \qquad N_{\text{comp}} = 0, \quad \text{for } |p| \in (0, p_c^-(\epsilon)) \text{ and } (p_c^+(\epsilon), p_0(\epsilon)),$$

where $p_c^{\pm}(\epsilon) = \frac{1}{2} + \mathcal{O}(\epsilon)$ as $\epsilon \to 0$. For these values of ϵ and p, the discrete line solitons are spectrally stable. It remains to show that

$$N_{\text{imag}}^- = 0 \quad \text{and} \quad N_{\text{comp}} = 1 \quad \text{for } |p| \in (p_c^-(\epsilon), p_c^+(\epsilon))$$

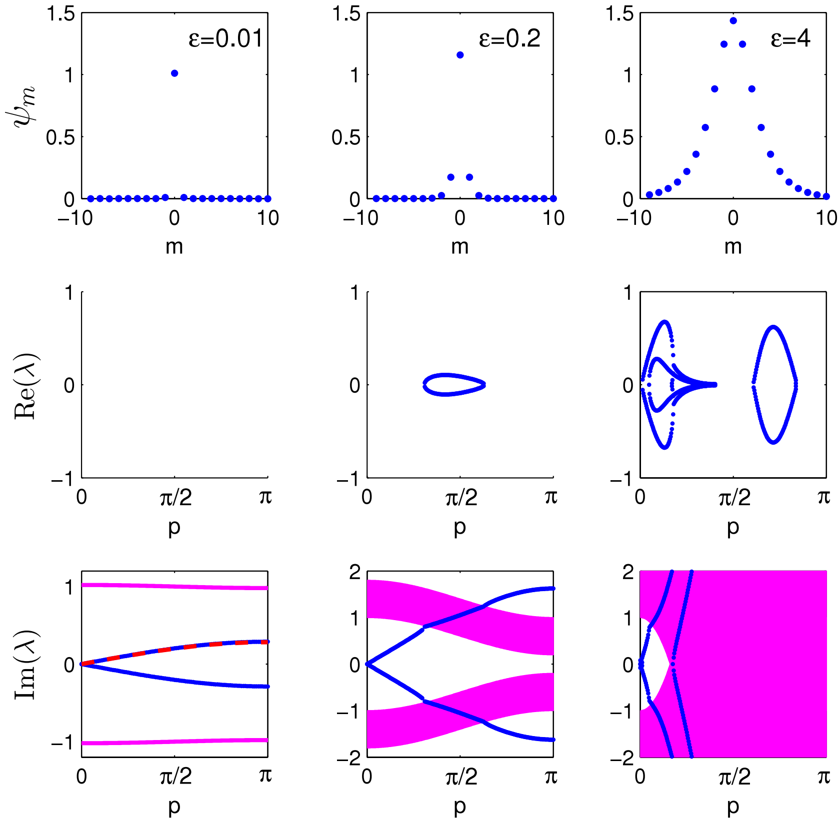

Fig. 2. Numerical results for discrete line solitons (2.15) bifurcating from the X point of the dNLS equation (2.1) on a two-dimensional lattice. Upper row: profiles of discrete line solitons ψ_m; middle row: real parts of eigenvalues λ of the spectral stability problem (2.16) versus the transverse wavenumber p; lower row: imaginary parts of eigenvalues λ versus p (the shaded pink region is the continuous spectrum). Left column: $\epsilon = 0.01$; middle column: $\epsilon = 0.2$; right column: $\epsilon = 4$. The red dashed line in the lower left panel is the leading-order analytical approximation (2.18) in Theorem 2.

due to a resonance between eigenvalues of negative and positive Krein signatures.

First we introduce a scaling transformation

$$p^2 = \frac{1}{4} + \epsilon\delta, \qquad \lambda = \frac{3i}{4} + i\epsilon\gamma,$$

$$U_m = \frac{a_m + b_m}{2}, \qquad W_m = \frac{a_m - b_m}{2i},$$

where $\delta, \gamma = \mathcal{O}(1)$. Under this transformation, the eigenvalue problem (3.4) for $\mu = 1$ and $\kappa = -1$ becomes

$$-\epsilon(a_{m+1} - 2a_m + a_{m-1}) - (1 + 2\epsilon)\delta_{m,0}(2a_0 + b_0) + \mathcal{O}(\epsilon^2)(2a_m + b_m) = \epsilon(\gamma + \delta)a_m, \quad (3.10)$$

$$-\epsilon(b_{m+1} - 2b_m + b_{m-1}) - (1 + 2\epsilon)\delta_{m,0}(a_0 + 2b_0) + \mathcal{O}(\epsilon^2)(a_m + 2b_m) = -\left(\frac{3}{2} + \epsilon\gamma - \epsilon\delta\right) b_m. \quad (3.11)$$

From the second equation (3.11), we obtain

$$b_0 = -2(1 - 2\epsilon + 2\epsilon\gamma - 2\epsilon\delta + \mathcal{O}(\epsilon^2))a_0, \quad (3.12)$$

whereas $b_{\pm m} = \mathcal{O}(\epsilon^m)b_0$ for any $m \in \mathbb{N}$. The first equation (3.10) for any $m \neq 0$ produces the second-order difference equation

$$-(a_{m+1} - 2a_m + a_{m-1}) + \mathcal{O}(\epsilon)a_m = (\gamma + \delta)a_m, \quad m \in \mathbb{Z} \setminus \{0\},$$

which admits a unique decaying solution for both $m \to \infty$ and $m \to -\infty$:

$$a_m = a_0 e^{-\rho|m|}, \quad m \in \mathbb{Z} \setminus \{0\},$$

where ρ is a unique root of the transcendent equation

$$\gamma + \delta = 2 - 2\cosh(\rho), \qquad \mathrm{Re}(\rho) > 0. \quad (3.13)$$

To obtain the value for ρ we close the first equation (3.10) at $m = 0$:

$$-2\epsilon(e^{-\rho} - 1)a_0 - (1 + 2\epsilon + \mathcal{O}(\epsilon^2))(2a_0 + b_0) = \epsilon(\gamma + \delta)a_0.$$

Utilizing (3.12), this equation becomes

$$-2(e^{-\rho} - 1) - 4(1 - \gamma + \delta) + \mathcal{O}(\epsilon) = \gamma + \delta.$$

Substituting (3.13) and neglecting the $\mathcal{O}(\epsilon)$ term, we convert this equation to a quadratic equation for $z = e^{\rho}$:

$$3z^2 + 4(2\delta - 1)z + 5 = 0,$$

which admits two possible solutions

$$z = \frac{2(1 - 2\delta) \pm i\sqrt{15 - 4(1 - 2\delta)^2}}{3}.$$

With the help of (3.13), these solutions produce expressions for γ as

$$\gamma = \frac{14 + 17\delta \mp i\sqrt{15 - 4(1 - 2\delta)^2}}{15},$$

which are complex-valued if $(1 - 2\delta)^2 < \frac{15}{4}$. These expressions yield the asymptotic approximations (3.7) and (3.8). From (3.8), we see that the most unstable eigenvalue occurs at $\delta = \frac{1}{2}$, which yields the asymptotic approximation (3.9). □

4. Numerical results

In this section, we present numerical results on transverse-stability eigenvalues of discrete line solitons in one- and two-dimensional lattices for various values of lattice coupling

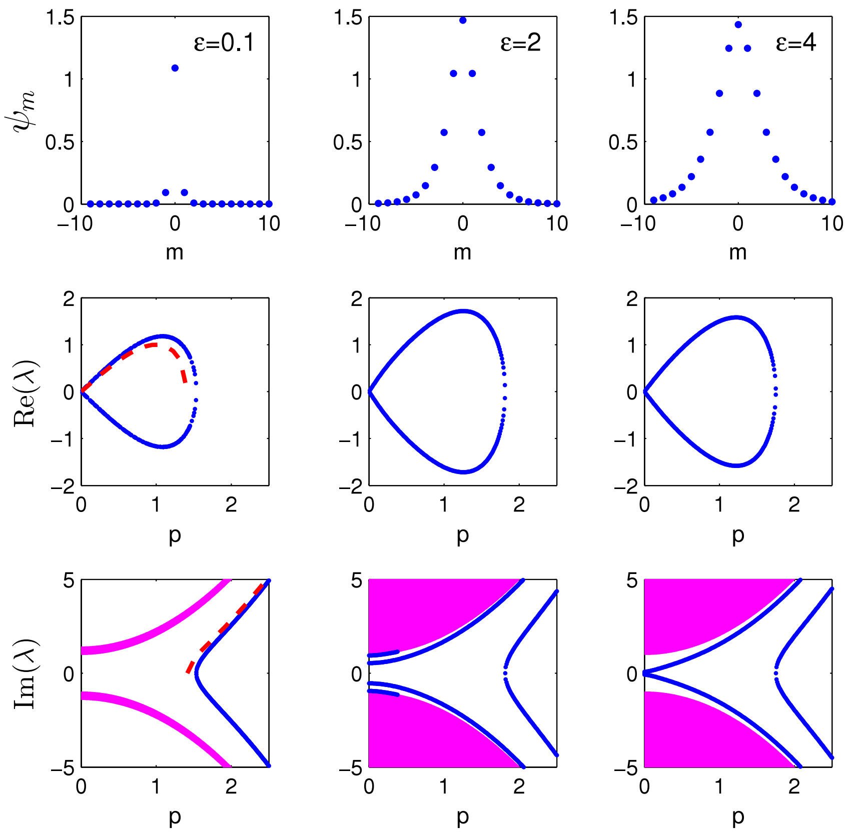

Fig. 3. Numerical results for discrete line solitons (3.3) in the dNLS equation (3.1) on a one-dimensional lattice with $\kappa = 1$. Upper row: profiles of discrete line solitons ψ_m; middle row: real parts of eigenvalues λ of the spectral stability problem (3.4) versus the transverse wavenumber p; lower row: imaginary parts of eigenvalues λ versus p (the shaded pink region is the continuous spectrum). Left column: $\epsilon = 0.1$; middle column: $\epsilon = 2$; right column: $\epsilon = 4$. The red dashed lines in the middle and lower left panels are the leading-order analytical approximations (3.6) in Theorem 3.

parameter ϵ (with fixed $\mu = 1$). These numerical results are shown to be in good agreement with the analytical results both qualitatively and quantitatively.

4.1. Numerical results for the dNLS equation on a two-dimensional lattice

First we consider discrete line solitons (2.8) bifurcating from the Γ point in the dNLS equation (2.1). At three values of ϵ, eigenvalues of the spectral stability problem (2.10) for various transverse wavenumbers p in the interval $[0, \pi]$ are presented in Fig. 1 (eigenvalues for negative p are the same as those for positive p). We see that when $\epsilon = 0.1$, a single pair of real eigenvalues exists for all values of p in $(0, \pi]$, in agreement with Theorem 1. These real eigenvalues closely match the asymptotic formula (2.13) in Theorem 1 (middle left panel). When $\epsilon = 1$, this pair of real eigenvalues exist only in the interval of $0 < p < p_0$, where $p_0 \approx 2.51$. For $p > p_0$, these real eigenvalues become purely imaginary. When $\epsilon = 4$, the p-interval of real eigenvalues further shrinks to $(0, p_0)$ with $p_0 \approx 0.91$. Meanwhile, an additional pair of imaginary discrete eigenvalues appear for all values of p in $[0, \pi]$. When $\epsilon \to +\infty$, the discrete line soliton ψ_m approaches the slowly-varying function (2.4) with $\mu = 1$, and the interval of real eigenvalues shrinks to $(0, p_0)$ with $p_0(\epsilon) \to \sqrt{3/\epsilon}$, according to the elliptic 2D NLS equation (2.6) (see [5] and [6, Section 5.9]).

Next we consider discrete line solitons (2.15) bifurcating from the X point in the dNLS equation (2.1). At three values of ϵ, eigenvalues of the spectral stability problem (2.16) for various transverse wavenumbers p in the interval $[0, \pi]$ are presented in Fig. 2. We see that when $\epsilon = 0.01$, a single pair of purely imaginary eigenvalues exists for all values of p in $(0, \pi]$, in agreement with Theorem 2. These imaginary eigenvalues match the asymptotic formula (2.18) in Theorem 2 (lower left panel). When $\epsilon = 0.2$, this pair of imaginary eigenvalues intersect the continuous spectrum (lower middle panel). As a consequence, complex eigenvalues appear on the p-interval of $0.97 < p < 1.97$ (center panel). When $\epsilon = 4$, additional eigenvalues exist. The eigenvalue curves on the left side of the p-interval (right middle and lower panels) are the counterparts of similar curves for line solitons in the hyperbolic 2D NLS equation (2.7) (see [30] and [6, Section 5.9]). But the curve of real eigenvalues on the right side of the p-interval (right middle panel) has no counterpart in the hyperbolic 2D NLS equation (2.7). These real eigenvalues bifurcate out from the origin inside the continuous spectrum. As $\epsilon \to +\infty$, the eigenvalue curves on the left side of the p-interval shrink towards $p = 0$ at the asymptotic rate of $\epsilon^{-1/2}$. Meanwhile, the real-eigenvalue curve on the right side of the p-interval approaches the edge point $p = \pi$, and its width shrinks at the asymptotic rate of $\epsilon^{-1/2}$.

4.2. Numerical results for the dNLS equation on a one-dimensional lattice

Now we consider discrete line solitons (3.3) in the dNLS equation (3.1) with $\kappa = 1$. At three values of ϵ, eigenvalues of the spectral stability problem (3.4) for various transverse wavenumbers p are presented in Fig. 3. We see that when $\epsilon = 0.1$, a pair of real eigenvalues exists in the interval $(0, p_0)$, where $p_0 \approx 1.53$. For $p > p_0$, these real eigenvalues become purely imaginary. This is in agreement with Theorem 3. Quantitatively, these real and imaginary eigenvalues are well approximated by the leading-order asymptotic formula (3.6) in Theorem 3. At $\epsilon = 2$, we still have the instability band $(0, p_0)$ with $p_0 \approx 1.81$. Meanwhile, two additional

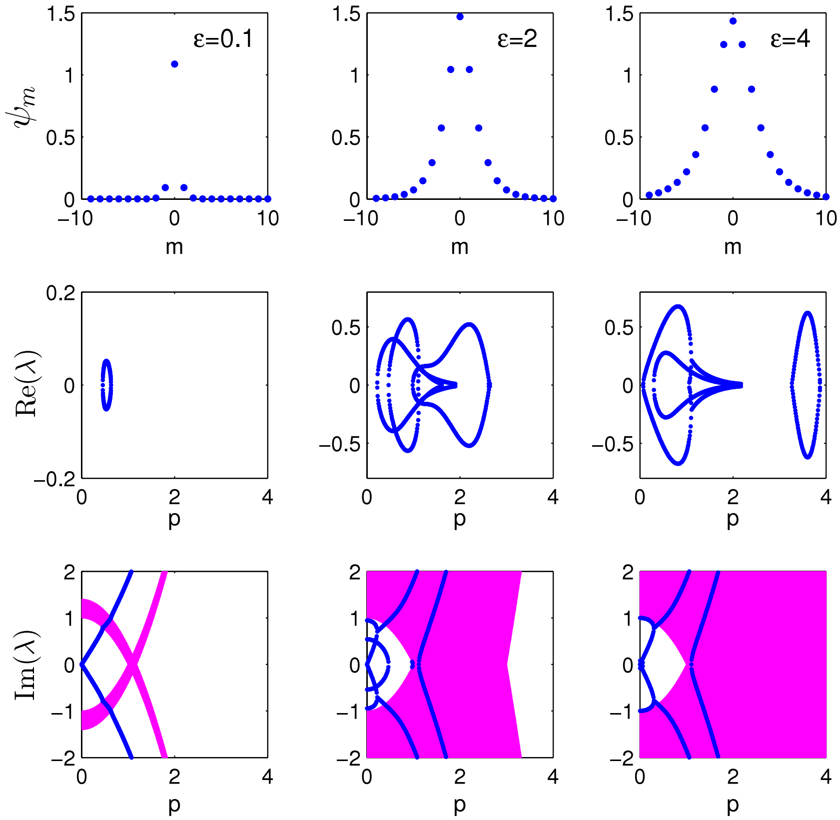

Fig. 4. Numerical results for discrete line solitons (3.3) in the dNLS equation (3.1) on a one-dimensional lattice with $\kappa = -1$. Upper row: profiles of discrete line solitons ψ_m; middle row: real parts of eigenvalues λ of the spectral stability problem (3.4) versus the transverse wavenumber p; lower row: imaginary parts of eigenvalues λ versus p (the shaded pink region is the continuous spectrum). Left column: $\epsilon = 0.1$; middle column: $\epsilon = 2$; right column: $\epsilon = 4$.

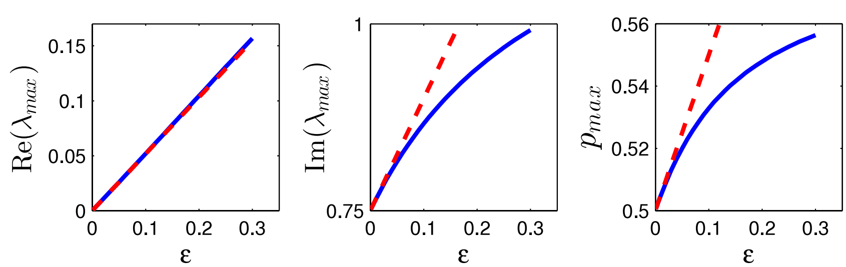

Fig. 5. The ϵ-dependence of the most unstable eigenvalue $\lambda_{\max}$ and its corresponding transverse wavenumber $p_{\max}$ for discrete line solitons (3.3) in the dNLS equation (3.1) with $\kappa = -1$. The red dashed lines are the leading-order analytical approximations (3.9) in Theorem 4.

branches of purely imaginary eigenvalues appear over certain p-intervals. When $\epsilon = 4$, the instability band $(0, p_0)$ has $p_0 \approx 1.75$, and one additional branch of purely imaginary eigenvalues exists over the entire p-axis. When $\epsilon \to +\infty$, $p_0(\epsilon) \to \sqrt{3}$ according to the elliptic 2D NLS equation (2.6) [5,6].

Next we consider discrete line solitons (3.3) in the dNLS equation (3.1) with $\kappa = -1$. At the same values of ϵ, eigenvalues of the spectral stability problem (3.4) for various transverse wavenumbers p are presented in Fig. 4. We see that when $\epsilon = 0.1$, a pair of imaginary eigenvalues intersect the continuous spectrum (lower left panel). As a consequence, complex eigenvalues bifurcate out near $p = 1/2$, in agreement with Theorem 4 (middle left panel). When $\epsilon = 2$, additional eigenvalue bifurcations occur (middle column). When $\epsilon = 4$, eigenvalue curves split into two parts. The left part is the counterpart of similar curves for line solitons in the hyperbolic 2D NLS equation (2.7) [30,6], while the right part is a curve of real eigenvalues at large p. Notice that this eigenvalue structure at $\epsilon = 4$ qualitatively resembles that in Fig. 2 (right column) for discrete line solitons bifurcated from the X point in the dNLS equation (2.1). As $\epsilon \to +\infty$, the left part of this structure asymptotically approaches eigenvalue curves for line solitons in the hyperbolic 2D NLS equation (2.7). On the other hand, the location of the right real-eigenvalue curve moves to $p \to \infty$ at the asymptotic rate of $\epsilon^{1/2}$, and its width shrinks at the asymptotic rate of $\epsilon^{-1/2}$.

Lastly, we quantitatively compare the numerical complex eigenvalues bifurcating from $p = 1/2$ with the analytical formulas for small ϵ in Theorem 4. For this purpose, we have numerically determined the most unstable complex eigenvalue $\lambda_{\max}$ and its p-location $p_{\max}$ for each ϵ in the range of $0 < \epsilon < 0.3$, and the results are displayed in Fig. 5. For comparison, the leading-order analytical approximations (3.9) for $\lambda_{\max}$ and $p_{\max}$ are also plotted in this figure. We can see that the analytical and numerical results closely match each other.

5. Summary and discussion

In this article, we have analytically determined the transverse stability and instability of line solitons in the discrete nonlinear

Schrödinger equations on one- and two-dimensional lattices in the anti-continuum limit. On a two-dimensional lattice, the fundamental line soliton was proved to be transversely stable (unstable) when it bifurcates from the X (Γ) point of the dispersion surface. On a one-dimensional (stripe) lattice, the fundamental line soliton was proved to be transversely unstable for both signs of transverse dispersion. In addition to these qualitative stability results, we have also derived asymptotic expressions for unstable eigenvalues and compared them with numerical results, and good agreements have been obtained.

It is noted that the discrete nonlinear Schrödinger equations are generally used to describe wave dynamics in the continuous NLS equations with a deep periodic potential and without inter-band mode coupling. Although the analytical results in this article nicely explained many of the numerical results on the transverse stability of line solitons in the continuous NLS equations [16,17], they cannot explain some other notable facts in the continuous models. For instance, our analytical results for the dNLS equation (3.1) on a one-dimensional lattice say that all line solitons are transversely unstable, but the numerical results in [17] showed that in the continuous model, line solitons near the second Bloch band can be transversely stable. The reason for this discrepancy is that line solitons near the second Bloch band contain a strong coupling between the first and second Bloch bands, which is neglected in the discrete NLS model. How to analytically explain the existence of transversely-stable line solitons in the continuous NLS equations with a one-dimensional lattice is still an open question which merits further study.

Acknowledgments

The work of DEP is supported in part by the NSERC and by the Ministry of Education and Science of Russian Federation (Project 14.B37.21.0868). The work of JY is supported in part by the Air Force Office of Scientific Research (Grant USAF 9550-12-1-0244) and the National Science Foundation (Grant DMS-0908167).

References

[1] V.E. Zakharov, A.M. Rubenchik, Instability of waveguides and solitons in nonlinear media, Sov. Phys. JETP 38 (1974) 494–500.
[2] N.N. Akhmediev, V.I. Korneev, R.F. Nabiev, Modulation instability of the ground state of the nonlinear wave equation: optical machine gun, Opt. Lett. 17 (1992) 393–395.
[3] A. De Rossi, S. Trillo, A.V. Buryak, Y.S. Kivshar, Symmetry-breaking instabilities of spatial parametric solitons, Phys. Rev. E 56 (1997) R4959–R4962.
[4] A. De Rossi, S. Trillo, A.V. Buryak, Y.S. Kivshar, Snake instability of one-dimensional parametric spatial solitons, Opt. Lett. 22 (1997) 868–870.
[5] Yu.S. Kivshar, D.E. Pelinovsky, Self-focusing and transverse instabilities of solitary waves, Phys. Rep. 331 (2000) 117–195.
[6] J. Yang, Nonlinear Waves in Integrable and Nonintegrable Systems, SIAM, Philadelphia, 2010.
[7] S.P. Gorza, Ph. Emplit, M. Haelterman, Observation of the snake instability of a spatially extended temporal bright soliton, Opt. Lett. 31 (2006) 1280–1282.
[8] S.P. Gorza, B. Deconinck, Ph. Emplit, T. Trogdon, M. Haelterman, Experimental demonstration of the oscillatory snake instability of the bright soliton of the (2 + 1)D hyperbolic nonlinear Schrödinger equation, Phys. Rev. Lett. 106 (2011) 094101.
[9] A.V. Mamaev, M. Saffman, A.A. Zozulya, Break-up of two-dimensional bright spatial solitons due to transverse modulation instability, Europhys. Lett. 35 (1996) 25–30.
[10] A.B. Aceves, C. De Angelis, G.G. Luther, A.M. Rubenchik, Modulational instability of continuous waves and one-dimensional temporal solitons in fiber arrays, Opt. Lett. 19 (1994) 1186–1188.
[11] D. Neshev, A.A. Sukhorukov, Y.S. Kivshar, W. Krolikowski, Observation of transverse instabilities in optically induced lattices, Opt. Lett. 29 (2004) 259–261.
[12] C. Anastassiou, M. Soljacic, M. Segev, E.D. Eugenieva, D.N. Christodoulides, D. Kip, Z.H. Musslimani, J.P. Torres, Eliminating the transverse instabilities of Kerr solitons, Phys. Rev. Lett. 85 (2000) 4888–4891.
[13] M. Ma, R. Carretero-Gonzáles, P.G. Kevrekidis, D.J. Frantzeskakis, B.A. Malomed, Controlling the transverse instability of dark solitons and nucleation of vortices by a potential barrier, Phys. Rev. A 82 (2010) 023621.
[14] Z.H. Musslimani, M. Segev, A. Nepomnyashchy, Y.S. Kivshar, Suppression of transverse instabilities for vector solitons, Phys. Rev. E 60 (1999) R1170–R1173.
[15] Z.H. Musslimani, J. Yang, Transverse instability of strongly coupled dark–bright Manakov vector solitons, Opt. Lett. 26 (2001) 1981–1983.
[16] J. Yang, Transversely stable soliton trains in photonic lattice, Phys. Rev. A 84 (2011) 033840.
[17] J. Yang, D. Gallardo, A. Miller, Z. Chen, Elimination of transverse instability in stripe solitons by one-dimensional lattices, Opt. Lett. 37 (2012) 1571–1573.
[18] Q.E. Hoq, J. Gagnon, P.G. Kevrekidis, B.A. Malomed, D.J. Franzeskakis, R. Carretero-Gonzáles, Extended nonlinear waves in multidimensional dynamical lattices, Math. Comput. Simul. 80 (2009) 721–731.
[19] P.G. Kevrekidis, J. Gagnon, D.J. Franzeskakis, B.A. Malomed, X, Y, and Z waves: extended structures in nonlinear lattices, Phys. Rev. E 75 (2007) 016607.
[20] M. Chugunova, D. Pelinovsky, Count of unstable eigenvalues in the generalized eigenvalue problem, J. Math. Phys. 51 (2010) 052901.
[21] T. Kapitula, P.G. Kevrekidis, B. Sandstede, Counting eigenvalues via the Krein signature in infinite-dimensional Hamiltonian systems, Physica D 195 (2004) 263–282; Addendum: Physica D 201 (2005) 199–201.
[22] D.E. Pelinovsky, Inertia law for spectral stability of solitary waves in coupled nonlinear Schrödinger equations, Proc. R. Soc. Lond. Ser. A 461 (2005) 783–812.
[23] R.S. MacKay, S. Aubry, Proof of existence of breathers for time-reversible or Hamiltonian networks of weakly coupled oscillators, Nonlinearity 7 (1994) 1623–1643.
[24] D.E. Pelinovsky, P.G. Kevrekidis, D.J. Frantzeskakis, Stability of discrete solitons in nonlinear Schrödinger lattices, Physica D 212 (2005) 1–19.
[25] P.G. Kevrekidis, The Discrete Nonlinear Schrödinger Equation: Mathematical Analysis, Numerical Computations and Physical Perspectives, Springer-Verlag, Heidelberg, 2009.
[26] D.E. Pelinovsky, Localization in Periodic Potentials: From Schrödinger Operators to the Gross–Pitaevskii Equation, Cambridge University Press, Cambridge, 2011.
[27] M. Herrmann, Homoclinic standing waves in focusing dNLS equations, Discrete Contin. Dyn. Syst. 31 (2011) 737–752.
[28] W.-X. Qin, X. Xiao, Homoclinic orbits and localized solutions in nonlinear Schrödinger lattices, Nonlinearity 20 (2007) 2305–2317.
[29] D. Bambusi, T. Penati, Continuous approximation of breathers in 1D and 2D dNLS lattices, Nonlinearity 23 (2010) 143–157.
[30] B. Deconinck, D. Pelinovsky, J.D. Carter, Transverse instabilities of deep-water solitary waves, Proc. R. Soc. A 462 (2006) 2039–2061.
[31] R.S. Hilscher, Spectral and oscillation theory for general second order Sturm–Liouville difference equations, Adv. Difference Equ. 2012 (2012) 82.
[32] A. Jirari, Second-order Sturm–Liouville difference equations and orthogonal polynomials, Memoirs AMS 542 (1995).
[33] D.E. Pelinovsky, A. Sakovich, Internal modes of discrete solitons near the anti-continuum limit of the dNLS equation, Physica D 240 (2011) 265–281.
[34] A.B. Aceves, G.G. Luther, C. De Angelis, A.M. Rubenchik, S.K. Turitsyn, Energy localization in nonlinear fiber arrays: collapse–effect compressor, Phys. Rev. Lett. 75 (1995) 73–76.
[35] A.B. Aceves, G.G. Luther, C. De Angelis, A.M. Rubenchik, S.K. Turitsyn, All-optical-switching and pulse amplification and steering in nonlinear fiber arrays, Physica D 87 (1995) 262–272.
[36] M.I. Weinstein, B. Yeary, Excitation and dynamics of pulses in coupled fiber arrays, Phys. Lett. A 222 (1996) 157–162.
[37] V. Vougalter, D. Pelinovsky, Eigenvalues of zero energy in the linearized NLS problem, J. Math. Phys. 47 (2006) 062701.